

Mass limits for the chiral color symmetry G' -boson from LHC dijet data

I. V. Frolov*, A. D. Smirnov†

Division of Theoretical Physics, Department of Physics,
Yaroslavl State University, Sovetskaya 14,
150000 Yaroslavl, Russia.

Abstract

The contributions of G' -boson predicted by the chiral color symmetry of quarks to the differential dijet cross-sections in pp -collisions at the LHC are calculated and analysed in dependence on two free parameters of the model, the G' mass $m_{G'}$ and mixing angle θ_G . The exclusion and consistency $m_{G'} - \theta_G$ regions imposed by the ATLAS and CMS data on dijet cross-sections are found. Using the CT10 (MSTW 2008) PDF set we show that the G' -boson for $\theta_G = 45^\circ$, i.e. the axigluon, with the masses $m_{G'} < 2.3$ (2.6) TeV and $m_{G'} < 3.35$ (3.25) TeV is excluded at the probability level of 95% by the ATLAS and CMS dijet data respectively. For the other values of θ_G the exclusion limits are more stringent. The $m_{G'} - \theta_G$ regions consistent with these data at $CL = 68\%$ and $CL = 90\%$ are also found.

Keywords: New physics; chiral color symmetry; axigluon; massive color octet; G' -boson; dijet cross section.

The search for the possible effects of new physics beyond the Standard Model (SM) is now one of the main goals of the experiments at the LHC. By now there are many models predicting new particles which can manifest themselves at the LHC energy through the possible new physics effects. Among such particles there are new quarks and leptons of the fourth generation of fermions, supersymmetric particles of the supersymmetry models, new scalar particles of two Higgs models, new gauge bosons of the weak left-right symmetry model, gauge and scalar leptoquarks of the four color quark-lepton symmetry models, etc. The unobservation of the new physics effects induced by these particles at the LHC will set new limits on the parameter of corresponding models.

One of such models which also predict new particles and can induce the new physics effects at the LHC energy is based on the gauge group of the chiral color symmetry of quarks

$$G_c = SU_{cL}(3) \times SU_{cR}(3) \xrightarrow{M_{chc}} SU_c(3) \quad (1)$$

which is assumed to be valid at high energies and is spontaneously broken to usual QCD $SU_c(3)$ at some low energy scale M_{chc} . The idea of the originally chiral character of $SU_c(3)$

*e-mail: pytnik89@mail.ru

†e-mail: asmirnov@uniyar.ac.ru

color symmetry of quarks was firstly proposed and realized for particular case of $g_L = g_R$ in refs. [1–4] and then it was extended to the more general case of $g_L \neq g_R$ [5–8].

The chiral color symmetry of quarks in addition to the usual gluons predicts immediately a new massive gauge particle – the axigluon G^A (in the case of $g_L = g_R$) with pure axial vector couplings to quarks or G' -boson (in the case of $g_L \neq g_R$) with vector and axial vector couplings to quarks defined by the gauge group (1). In both cases this new particle interacts with quarks with coupling constants of order g_{st} and can induce appreciable effects in the processes with quarks. In particular G' -boson could give rise at the LHC to the charge asymmetry of $t\bar{t}$ production as well as to the appearance of a resonant peak in the invariant mass spectrum of dijet events. The possible effect of G' -boson on the charge asymmetry of $t\bar{t}$ production at the LHC (and at the Tevatron) and the corresponding G' -boson mass limits have been discussed in [6–9].

In the present paper we calculate and analyse the possible G' -boson contributions to the differential dijet cross-sections in pp -collisions at the LHC in comparison with the ATLAS [10] and CMS [11, 12] data on dijet cross-sections and find the G' -boson mass limits imposed by these experimental data.

The basic gauge fields of the group (1) G_μ^L and G_μ^R form the usual gluon field G_μ and the field G'_μ of an additional G' -boson as superpositions

$$G_\mu = \frac{g_R G_\mu^L + g_L G_\mu^R}{\sqrt{(g_L)^2 + (g_R)^2}} \equiv s_G G_\mu^L + c_G G_\mu^R, \quad (2)$$

$$G'_\mu = \frac{g_L G_\mu^L - g_R G_\mu^R}{\sqrt{(g_L)^2 + (g_R)^2}} \equiv c_G G_\mu^L - s_G G_\mu^R, \quad (3)$$

where $G_\mu^{L,R} = G_{i\mu}^{L,R} t_i$, $G_\mu = G_\mu^i t_i$, $G'_\mu = G'_\mu^i t_i$, $i = 1, 2, \dots, 8$, t_i are the generators of $SU_c(3)$ group, $s_G = \sin \theta_G$, $c_G = \cos \theta_G$, θ_G is $G^L - G^R$ mixing angle, $\tan \theta_G = g_R/g_L$ and g_L, g_R are the coupling constants of the group (1).

The interaction of the G' -boson with quarks can be written as

$$\mathcal{L}_{G'qq} = g_{st}(M_{chc}) \bar{q} \gamma^\mu (v + a \gamma_5) G'_\mu q, \quad (4)$$

where

$$g_{st}(M_{chc}) = \frac{g_L g_R}{\sqrt{(g_L)^2 + (g_R)^2}}$$

is the strong interaction coupling constant at the mass scale M_{chc} of the chiral color symmetry breaking and the vector and axial-vector coupling constants v and a are defined by the group (1) and with account of the relations (2), (3) take the form

$$v = \frac{c_G^2 - s_G^2}{2s_G c_G} = \cot(2\theta_G), \quad a = \frac{1}{2s_G c_G} = 1/\sin(2\theta_G). \quad (5)$$

After spontaneously breaking the symmetry (1) the G' -boson acquires some mass $m_{G'}$ and as a result we obtain two free parameters in the model, the G' -boson mass $m_{G'}$ and the $G^L - G^R$ mixing angle θ_G . For $g_L = g_R$ we have $\theta_G = 45^\circ$, $v = 0$, $a = 1$ and G' -boson in this case coincides with the axigluon.

The interaction (4) gives to the G' -boson the hadronic width

$$\Gamma_{G'} = \sum_Q \Gamma(G' \rightarrow Q\bar{Q}), \quad (6)$$

where

$$\Gamma(G' \rightarrow Q\bar{Q}) = \frac{\alpha_s m_{G'}}{6} \left[v^2 \left(1 + \frac{2m_Q^2}{m_{G'}^2} \right) + a^2 \left(1 - \frac{4m_Q^2}{m_{G'}^2} \right) \right] \sqrt{1 - \frac{4m_Q^2}{m_{G'}^2}} \quad (7)$$

is the width of G' -boson decay into $Q\bar{Q}$ -pair. From (5)–(7) follow the next estimations for the relative width of G' -boson $\Gamma_{G'}/m_{G'} = 0.11, 0.18, 0.41, 0.75, 1.71$ for $\theta_G = 45^\circ, 30^\circ, 20^\circ, 15^\circ, 10^\circ$ respectively.

The chiral color symmetry of quarks needs the extensions of the fermion sector of the model for cancellations of the chiral γ_5 -anomalies which are produced by quarks in the case of the chiral color symmetry (1) as well as of the scalar one for giving necessary masses to the fermions and gauge particles of the model. For discussing these extensions the chiral color symmetry (1) should be unified with the electroweak $SU_L(2) \times U(1)$ symmetry of the SM for example in the simplest way by the group

$$G_{3321} = SU_{cL}(3) \times SU_{cR}(3) \times SU_L(2) \times U(1), \quad (8)$$

where the first two factors are given by the group (1) and the second ones form the usual SM electroweak symmetry group.

There are many approaches for cancellation of the chiral γ_5 -anomalies produced by the SM fermions through extensions of the SM fermion sector by introducing additional exotic fermions. The most simple and natural looks the variant [13] in which in the case of the group (8) for each SM doublet q of quarks $q_a, a = 1, 2$ transforming under the group (8) in the usual way

$$q^L : \quad (3, 1, 2, Y_{q^L}), \quad (9)$$

$$q_a^R : \quad (1, 3, 1, Y_{q_a^R}) \quad (10)$$

with the SM quark hypercharges $Y_{q^L} = 1/3, Y_{q_1^R} = 4/3, Y_{q_2^R} = -2/3$ one needs in each generation the existence of two exotic quarks \tilde{q}_a transforming under the group (8) as

$$\tilde{q}_a^L : \quad (1, 3, 1, Y_{\tilde{q}_a}), \quad (11)$$

$$\tilde{q}_a^R : \quad (3, 1, 1, Y_{\tilde{q}_a}), \quad (12)$$

where $Y_{\tilde{q}_1} = \tilde{Y}, Y_{\tilde{q}_2} = -\tilde{Y} + 2/3$ are the hypercharges of the exotic quarks, \tilde{Y} is an arbitrary hypercharge. With particular choice of $\tilde{Y} = 4/3$ the electric charges of the exotic quarks become the same as those of the SM quarks.

Using the transformation laws (11), (12) and the relations (2), (3) one can obtain the interaction of the exotic quarks with the G' -boson in the form

$$\mathcal{L}_{G'\tilde{q}\tilde{q}} = g_{st}(M_{chc}) \bar{\tilde{q}} \gamma^\mu (v - a\gamma_5) G'_\mu \tilde{q}, \quad (13)$$

where the constants v and a are given by the expressions (5). Additionally the exotic quarks have the vector-like interactions with the photon and SM Z -boson. As seen from (13) the axial-vector coupling constant of the exotic quarks with the G' -boson has the opposite sign relatively to that of the SM quarks, which ensures the cancellation of the chiral γ_5 -anomalies in diagrams with the G' -bosons.

For giving necessary masses to the fermions and gauge particles the scalar sector of the model should be appropriately extended. The masses to the usual quarks and leptons

can be given by the scalar doublets $(\Phi_a^{(1,2)})_{\alpha\beta}$ and $\Phi_a^{(3)}$ transforming under the group (8) as

$$(\Phi_a^{(1)})_{\alpha\beta} : \quad (3, \bar{3}, 2, -1), \quad (14)$$

$$(\Phi_a^{(2)})_{\alpha\beta} : \quad (3, \bar{3}, 2, +1), \quad (15)$$

$$\Phi_a^{(3)} : \quad (1, 1, 2, +1) \quad (16)$$

with VEVs $\langle(\Phi_a^{(b)})_{\alpha\beta}\rangle = \delta_{\alpha\beta} \delta_{ab} \eta_b / (2\sqrt{3})$ for $b = 1, 2$ and $\langle\Phi_a^{(3)}\rangle = \delta_{\alpha\beta} \eta_3 / \sqrt{2}$, $a = 1, 2$ is the $SU_L(2)$ index and $\alpha, \beta = 1, 2, 3$ are the $SU_{cL}(3)$ and $SU_{cR}(3)$ indices.

The mass to the G' -boson can be given by the scalar field $\Phi_{\alpha\beta}^{(0)}$ transforming under the group (8) as

$$(\Phi^{(0)})_{\alpha\beta} : \quad (3, \bar{3}, 1, 0) \quad (17)$$

with VEV $\langle\Phi_{\alpha\beta}^{(0)}\rangle = \delta_{\alpha\beta} \eta_0 / (2\sqrt{3})$. After such symmetry breaking the G' -boson acquires the mass

$$m_{G'} = \frac{g_{st}}{s_{GG}} \frac{\sqrt{\eta_1^2 + \eta_2^2 + \eta_0^2}}{\sqrt{6}}. \quad (18)$$

The field $\Phi_{\alpha\beta}^{(0)}$ can interact with the exotic quarks as

$$\mathcal{L}_{\Phi^{(0)}\tilde{q}\tilde{q}} = \tilde{q}_{ia\alpha}^R (h_a)_{ij} (\Phi^{(0)})_{\alpha\beta} \tilde{q}_{ja\beta}^L + \tilde{q}_{ia\alpha}^L (h_a^+)_{ij} ((\Phi^{(0)})^+)_{\alpha\beta} \tilde{q}_{ja\beta}^R, \quad (19)$$

where $(h_a)_{ij}$ form the matrices of Yukawa coupling constants, i, j are the generation indeces. By biunitary transformations these matrices can be reduced to the diagonal form $(h_{ia})\delta_{ij}$ and after the symmetry breaking the mass eigenstates \tilde{q}'_{ia} of the exotic quarks pick up the masses

$$m_{\tilde{q}'_{ia}} = h_{ia} \frac{\eta_0}{2\sqrt{3}}. \quad (20)$$

As a result of the decomposition $(3_L, \bar{3}_R) = 1_{SU_c(3)} + 8_{SU_c(3)}$ of the representation $(3_L, \bar{3}_R)$ of the group (1) the multiplets $(\Phi_a^{(1,2)})_{\alpha\beta}$ and $\Phi_{\alpha\beta}^{(0)}$ after the chiral color symmetry breaking give the color singlets $(\Phi_a^{(1,2;0)})_{\alpha\beta} = \Phi_{0a}^{(1,2)} \delta_{\alpha\beta} / \sqrt{6}$ and $\Phi_{\alpha\beta}^{(0;0)} = \Phi_0^{(0)} \delta_{\alpha\beta} / \sqrt{6}$ as well as the $SU_c(3)$ octets $(\Phi_a^{(1,2;8)})_{\alpha\beta} = \Phi_{ia}^{(1,2)}(t_i)_{\alpha\beta}$, $\Phi_{\alpha\beta}^{(0;8)} = \Phi_i^{(0)}(t_i)_{\alpha\beta}$. The color singlets $\Phi_{0a}^{(1,2)}$ and $\Phi_a^{(3)}$ are the $SU_L(2)$ doublets. These doublets are mixed and form the SM Higgs doublet $\Phi_a^{(SM)}$ with the SM VEV $\eta_{SM} = \sqrt{\eta_1^2 + \eta_2^2 + \eta_3^2} \approx 250 \text{ GeV}$ and two additional doublets Φ'_a , Φ''_a . As a result the chiral color symmetry reproduces in the scalar sector the SM Higgs doublet $\Phi_a^{(SM)}$ and predicts the new scalar fields: two colorless doublets Φ'_a and Φ''_a , two doublets of color octets $\Phi_{ia}^{(1,2)}$, the color octet $\Phi_i^{(0)}$ and the colorless $SU_L(2)$ singlet $\Phi_0^{(0)}$ with the VEV η_0 . The interactions of the doublet $\Phi_a^{(SM)}$ with the SM quarks and leptons and with W^\pm and Z bosons have the standard form.

The differential cross section of the process $pp \rightarrow cd + X$ of the inclusive production of two partons c and d in pp collisions can be written in the usual way as

$$d\sigma(pp \rightarrow cd + X) = \sum_{ab} \int \int f_a^p(x_1; \mu_F) f_b^p(x_2; \mu_F) d\sigma(ab \rightarrow cd) dx_1 dx_2, \quad (21)$$

where $a = q_i, \bar{q}_i, g$; $b = q_j, \bar{q}_j, g$ are the initial partons, $i, j = 1, 2, \dots, 5$ are the quark (or antiquark) flavour indices, $f_a^p(x; \mu_F)$ are the parton distribution function (PDF) of quark,

antiquark or gluon, $x_{1,2}$ are the momentum fractions of proton carried by initial partons, μ_F is the factorization scale and

$$d\sigma(ab \rightarrow cd) = (2\pi)^4 \delta^{(4)}(p_3 + p_4 - p_1 - p_2) \frac{|M_{ab \rightarrow cd}|^2}{2\hat{s}} \frac{d^3 p_3}{2E_3(2\pi)^3} \frac{d^3 p_4}{2E_4(2\pi)^3} \quad (22)$$

are the parton differential cross sections, $p_{1,2}$ and $p_{3,4} = \{E_{3,4}, \vec{p}_{3,4}\}$ are the four momenta of the initial and final partons, $\hat{s} = (p_1 + p_2)^2$.

The amplitudes of parton processes $ab \rightarrow cd$ can be presented as

$$M_{ab \rightarrow cd} = M_{ab \rightarrow cd}^{SM} + M_{ab \rightarrow cd}^{G',LO}, \quad (23)$$

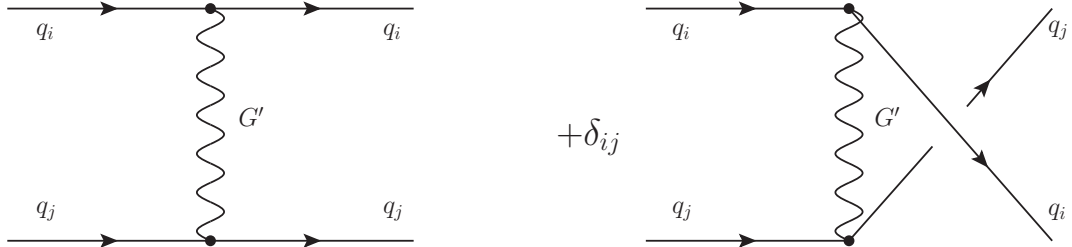
where

$$M_{ab \rightarrow cd}^{SM} = M_{ab \rightarrow cd}^{SM,LO} + M_{ab \rightarrow cd}^{SM,NLO} \quad (24)$$

are the SM amplitudes calculated up to next to leading order and the amplitudes $M_{ab \rightarrow cd}^{G',LO}$ give the G' -boson contributions in the leading order.

The amplitudes $M_{ab \rightarrow cd}^{G',LO}$ are described by the diagrams shown in the Fig. 1.

$$q_i(p_1)q_j(p_2) \rightarrow q_i(p_3)q_j(p_4) :$$



$$q_i(p_1)\bar{q}_j(p_2) \rightarrow q_k(p_3)\bar{q}_l(p_4) :$$

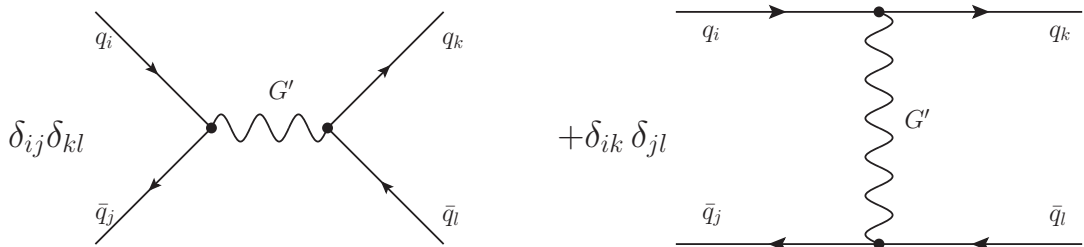


Figure 1: Diagrams describing the leading-order G' -boson contributions to the amplitudes $M_{ab \rightarrow cd}^{G',LO}$ of the partonic processes $q_i q_j \rightarrow q_i q_j$ and $q_i \bar{q}_j \rightarrow q_k \bar{q}_l$ (diagrams for the processes $\bar{q}_i \bar{q}_j \rightarrow \bar{q}_i \bar{q}_j$ can be obtained from the diagrams of the processes $q_i q_j \rightarrow q_i q_j$ by changing the directions of the fermion lines)

For the squared amplitudes $|M_{ab \rightarrow cd}|^2$ we use the expressions

$$|M_{ab \rightarrow cd}|^2 = |M_{ab \rightarrow cd}^{SM}|^2 + |M_{ab \rightarrow cd}^{G',LO}|^2 + 2\text{Re}(M_{ab \rightarrow cd}^{SM,LO} M_{ab \rightarrow cd}^{G',LO}) + \dots, \quad (25)$$

where the dots denote the terms $2\text{Re}(M_{ab \rightarrow cd}^{SM,NLO} M_{ab \rightarrow cd}^{G',LO})$ omitted because of their smallness.

For the calculation of the G' -boson contribution in dijet mass spectrum we use a package for calculation of Feynman diagrams and integration over multi-particle phase space CalcHEP [14] and for calculation of differential dijet NLO cross section in the SM we use the program for computation of inclusive jet cross sections at hadron colliders MEKS [15].

As a result of calculations for the terms $|M_{ab \rightarrow cd}^{G',LO}|^2$ and $2Re(M_{ab \rightarrow cd}^{SM,LO} M_{ab \rightarrow cd}^{G',LO})$ in (25) we obtain the expressions

$$|M_{q_i q_j \rightarrow q_i q_j}^{G',LO}|^2 = |M_{\bar{q}_i \bar{q}_j \rightarrow \bar{q}_i \bar{q}_j}^{G',LO}|^2 = \frac{4g_{st}^4(M_{chc})}{27} \left(\frac{3\delta_{ij}(\hat{t}^2 A^2 + \hat{s}^2 B)}{(\hat{u} - m_{G'}^2)^2} - \frac{2\delta_{ij}\hat{s}^2 B}{(\hat{t} - m_{G'}^2)(\hat{u} - m_{G'}^2)} + \frac{3(\hat{u}^2 A^2 + \hat{s}^2 B)}{(\hat{t} - m_{G'}^2)^2} \right), \quad (26)$$

$$|M_{q_i \bar{q}_j \rightarrow q_k \bar{q}_l}^{G',LO}|^2 = \frac{4g_{st}^4(M_{chc})}{27} \left(\frac{3\delta_{ik}\delta_{jl}(\hat{s}^2 A^2 + \hat{u}^2 B)}{(\hat{t} - m_{G'}^2)^2} - \frac{2\delta_{ij}\delta_{jk}\hat{u}^2(\hat{s} - m_{G'}^2)B}{((\hat{s} - m_{G'}^2)^2 + m_{G'}^2\Gamma_{G'}^2)(\hat{t} - m_{G'}^2)} + \frac{3\delta_{ij}\delta_{kl}(\hat{t}^2 A^2 + \hat{u}^2 B)}{(\hat{s} - m_{G'}^2)^2 + m_{G'}^2\Gamma_{G'}^2} \right) \quad (27)$$

and

$$2Re(M_{q_i q_j \rightarrow q_i q_j}^{SM,LO} M_{q_i q_j \rightarrow q_i q_j}^{G',LO}) = 2Re(M_{\bar{q}_i \bar{q}_j \rightarrow \bar{q}_i \bar{q}_j}^{SM,LO} M_{\bar{q}_i \bar{q}_j \rightarrow \bar{q}_i \bar{q}_j}^{G',LO}) = \frac{8g_{st}^2(\mu_R)g_{st}^2(M_{chc})}{27} \left(\frac{3\hat{u}^3 A + \hat{s}^2(3\hat{u} - \delta_{ij}\hat{t})C}{\hat{t}\hat{u}(\hat{t} - m_{G'}^2)} + \frac{\delta_{ij}(3\hat{t}^3 A + \hat{s}^2(3\hat{t} - \hat{u})C)}{\hat{t}\hat{u}(\hat{u} - m_{G'}^2)} \right), \quad (28)$$

$$2Re(M_{q_i \bar{q}_j \rightarrow q_k \bar{q}_l}^{SM,LO} M_{q_i \bar{q}_j \rightarrow q_k \bar{q}_l}^{G',LO}) = \frac{8g_{st}^2(\mu_R)g_{st}^2(M_{chc})}{27} \left(\frac{\delta_{jl}(3\delta_{ik}\hat{s}^3 A + \hat{u}^2(3\delta_{ik}\hat{s} - \delta_{ij}\delta_{jk}\hat{t})C)}{\hat{s}\hat{t}(\hat{t} - m_{G'}^2)} + \frac{(\hat{s} - m_{G'}^2)(\hat{u}^2(3\delta_{ij}\delta_{kl}\hat{t} - \delta_{ij}\delta_{jk}\hat{s})C + 3\delta_{ij}\delta_{kl}\hat{t}^3 A)}{\hat{s}\hat{t}((\hat{s} - m_{G'}^2)^2 + m_{G'}^2\Gamma_{G'}^2)} \right), \quad (29)$$

where $A = (v^2 - a^2)$, $B = (a^4 + 6a^2v^2 + v^4)$, $C = (v^2 + a^2)$ and $\hat{s} = (p_1 + p_2)^2$, $\hat{t} = (p_1 - p_3)^2$, $\hat{u} = (p_2 - p_3)^2$, μ_R is the renormalization scale.

In order to compare the cross-section defined by the equations (21)–(29) with the experimental dijet double-differential cross-sections measured by the ATLAS collaboration [10] we have calculated the double-differential cross-sections averaged over the bins of ref. [10] as

$$\frac{\overline{d^2\sigma(pp \rightarrow \text{jet jet})}}{dm_{jj}d|y_*|} = \frac{1}{\Delta m_{jj}} \frac{1}{\Delta|y_*|} \int_{m_{jj}^-}^{m_{jj}^+} \int_{|y_*|^-}^{|y_*|^+} \frac{d^2\sigma(pp \rightarrow \text{jet jet})}{dm_{jj}d|y_*|} dm_{jj} d|y_*|, \quad (30)$$

where $m_{jj}^\pm = m_{jj} \pm \Delta m_{jj}/2$, $|y_*|^\pm = |y_*| \pm \Delta|y_*|/2$, m_{jj} ($|y_*|$) and Δm_{jj} ($\Delta|y_*|$) are the central value and the width of the invariant mass (half the rapidity separation) bin. The dijet double-differential cross-section $\frac{d^2\sigma(pp \rightarrow \text{jet jet})}{dm_{jj}d|y_*|}$ in (30) has been calculated from the cross-section (21), (22) with $|M_{ab \rightarrow cd}|^2$ defined by the equations (25)–(29) by using the package CalcHEP [14] and the program MEKS [15] with account the kinematic relations

$$\hat{s} = x_1 x_2 s, \quad \hat{t} = -\frac{\hat{s}}{2}(1 - \tanh(y_*)), \quad \hat{u} = -\frac{\hat{s}}{2}(1 + \tanh(y_*)), \quad (31)$$

$$y_* = \frac{y_3 - y_4}{2}, \quad y_{3,4} = \frac{1}{2} \ln \frac{E_{3,4} + p_{3,4;z}}{E_{3,4} - p_{3,4;z}}, \quad (32)$$

where \sqrt{s} is the center of mass energy of colliding protons, $y_{3,4}$ are the rapidities of the final partons and $m_{jj} = \hat{s} = x_1 x_2 s$ is the invariant mass of two jets.

For comparing the cross-section (21)–(29) with the experimental dijet differential cross-sections measured by the CMS collaboration [11] we have calculated the differential cross-sections averaged over the bins of ref. [11] as

$$\frac{d\sigma(pp \rightarrow \text{jet jet})}{dm_{jj}} = \frac{1}{\Delta m_{jj}} \int_{m_{jj}^-}^{m_{jj}^+} \int_0^{|\eta_*|_{max}} \frac{d^2\sigma(pp \rightarrow \text{jet jet})}{dm_{jj} d|\eta_*|} d|\eta_*|, \quad (33)$$

where the dijet double-differential cross-section $\frac{d^2\sigma(pp \rightarrow \text{jet jet})}{dm_{jj} d|\eta_*|}$ in (33) is obtained from $\frac{d^2\sigma(pp \rightarrow \text{jet jet})}{dm_{jj} d|y_*|}$ in (30) by the substitution $y_* \rightarrow \eta_*$ with

$$\eta_* = \frac{\eta_3 - \eta_4}{2}, \quad \eta_{3,4} = -\ln[\tan(\theta_{3,4}/2)],$$

where $\eta_{3,4}$ and $\theta_{3,4}$ are the pseudorapidities and the polar scattering angles of the final jets. The upper limit $|\eta_*|_{max}$ in (33) is defined by the CMS experiment. The variable $|\eta_*|$ relates to the pseudorapidity separation $|\Delta\eta_{jj}|$ used in ref. [11] as $|\Delta\eta_{jj}| = 2|\eta_*|$.

For the comparison of the experimental and theoretical results we use the variable χ_r^2 („reduced” χ^2) defined as

$$\chi_r^2 = \frac{1}{n} \sum_i^N \frac{(\sigma_i^{exp} - \sigma_i^{th})^2}{(\Delta\sigma_i^{exp})^2},$$

where σ_i^{exp} denote the experimental value of $\frac{d^2\sigma(pp \rightarrow \text{jet jet})}{dm_{jj} d|y_*|}$ in the case of the ATLAS data (or $\frac{d\sigma(pp \rightarrow \text{jet jet})}{dm_{jj}}$ in the case of the CMS data) in the i -th bin, σ_i^{th} is the corresponding theoretical value, $\Delta\sigma_i^{exp}$ is the experimental error of this value, $n = N - N_p$ is the number of degrees of freedom, N is the number of the bins under consideration and N_p is the number of the free parameters of the model. In the further analysis we use the values $N_p = 0$ for the SM and $N_p = 2$ for the gauge chiral color symmetry model.

The ATLAS dijet double-differential cross-sections were measured [10] for pp collisions at $\sqrt{s} = 7$ TeV with 4.5 fb^{-1} as functions of the dijet mass m_{jj} and half the rapidity separation $y^* = |y_3 - y_4|/2$ of the two leading jets (the variable y^* of ref. [10] relates to our variable (32) as $y^* = |y_*|$). The measurements are performed in six ranges of y^* in interval $0 < y^* < 3.0$ in equal steps of 0.5. The ATLAS collaboration provides the results as tables of measured dijet cross-section in $N = 21$ dijet mass bins for all six ranges of y^* .

In order to compare our results with the ATLAS measurements we have calculated the double-differential cross-sections (30) for the same dijet mass bins and the ranges of y^* as the ATLAS ones and use in our calculations the ATLAS kinematic cuts on the final states

$$\begin{aligned} |y_i| &< 3 \quad (i = 3, 4), \\ p_{T_i} &> 100 \text{ GeV}, \end{aligned}$$

where y_i and p_{T_i} are the rapidity and transverse momentum of each jet. We set also the factorization (μ_F) and renormalization (μ_R) scales as $\mu = \mu_R = \mu_F = p_T^{max} e^{0.3y^*}$ where p_T^{max} is the p_T of the leading jet. In the ATLAS analysis [10] the jets are clustered by the

anti- k_t algorithm using two values of the radius parameter, $R = 0.4$ and $R = 0.6$. For definiteness we perform our calculations and analysis of the ATLAS data with the value $R = 0.6$. To demonstrate the dependence of the results on the parton distribution functions we use in our theoretical evaluations two PDF sets, CT10 [17] and MSTW 2008 [16].

We have calculated the double-differential cross-sections (30) by means of the programs `MEKS` and `CalcHEP` with using the CT10 and MSTW 2008 PDF sets with account of the contributions of the SM NLO QCD and G' -boson in each dijet mass bin and in all the ranges of y^* for the model parameters $m_{G'} > 1$ TeV and $10^\circ < \theta_G < 45^\circ$. The results accounting only the SM NLO QCD contribution are in good agreement with the cross-sections measured by the ATLAS (in all the bins the theoretical cross-sections consist with the experimental ones within the experimental errors). For example, for the range $0 \leq y^* < 0.5$ and the jet radius parameter $R = 0.6$ we obtain that $\chi^2_{rSM} = 6.8/21 = 0.32$ in the case of using the CT10 PDF set and $\chi^2_{rSM} = 15.5/21 = 0.74$ in the case of the MSTW 2008 PDF set.

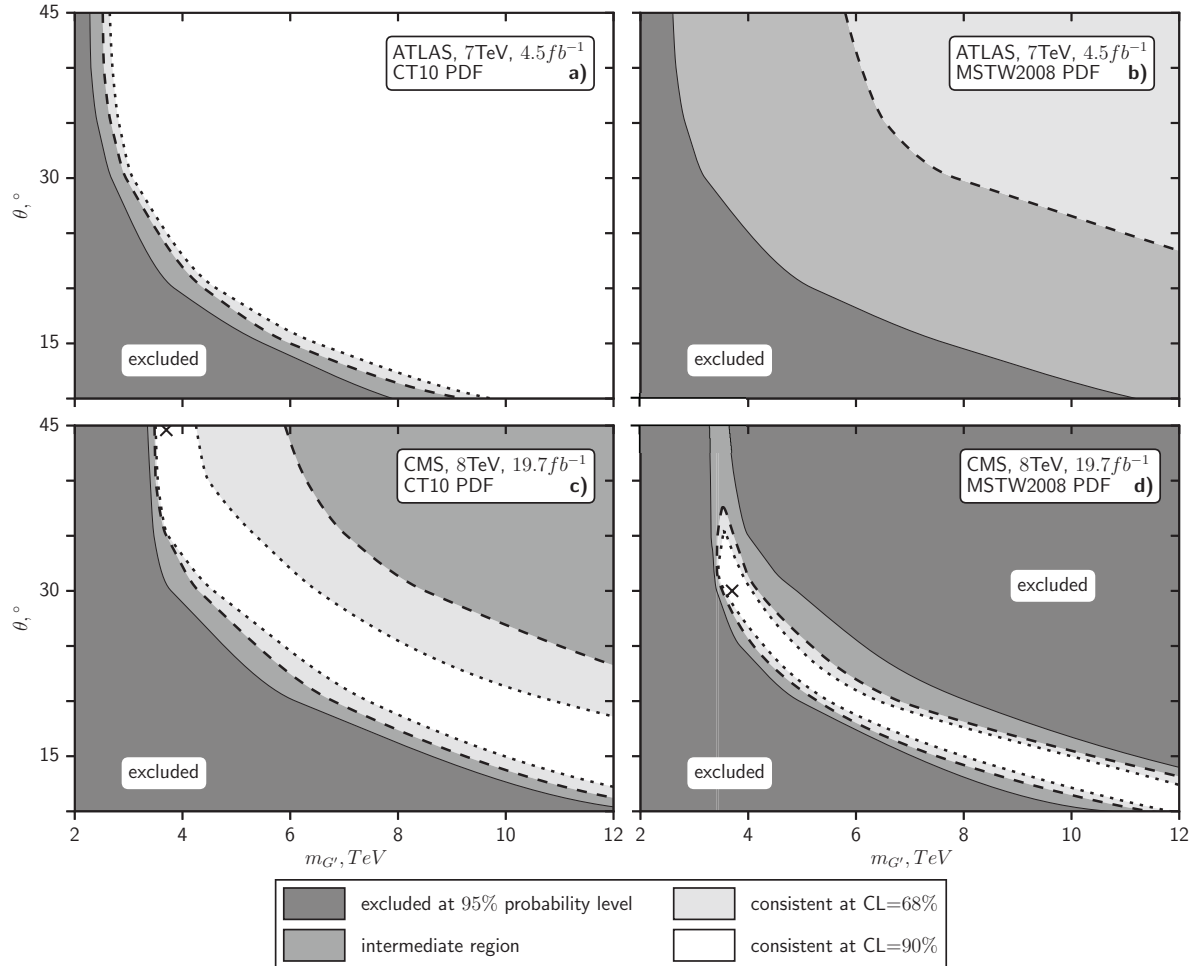


Figure 2: The exclusion (at 95% probability level) and consistency (at $CL = 68\%$ and $CL = 90\%$) $m_{G'} - \theta_G$ regions resulting from the ATLAS ($\sqrt{s} = 7$ TeV with 4.5 fb^{-1}) and CMS ($\sqrt{s} = 8$ TeV with 19.7 fb^{-1}) data on dijet cross sections with using the CT10 and MSTW 2008 PDF sets.

We have compared the results accounting simultaneously the contributions of the SM NLO QCD and G' -boson with the ATLAS data to find the regions of the parameters $m_{G'}$ and θ_G which are excluded by the ATLAS data at the appropriate level as well as the allowed ones.

In the upper sections of the Fig. 2 we show the excluded and allowed $m_{G'} - \theta_G$ regions resulting from the ATLAS data on the double-differential dijet cross sections for the range $0 \leq y^* < 0.5$ and the jet radius parameter $R = 0.6$ in the cases of using the CT10 (section a)) and MSTW 2008 (section b)) PDF sets. The solid line shows the bound of the $m_{G'} - \theta_G$ region excluded at the probability level of 95% and the dashed and dotted lines show the bounds of $m_{G'} - \theta_G$ regions which are consistent with the data at $CL = 68\%$ and $CL = 90\%$ respectively.

As seen from the Fig. 2 a), b) in the case of using the CT10 (MSTW 2008) PDF set the G' -boson for $\theta_G = 45^\circ$ (i.e. the axigluon) with the masses

$$m_{G'} < 2.3 \text{ (2.6) TeV} \quad (34)$$

is excluded at the probability level of 95% by the ATLAS dijet data and for the other values of θ_G the corresponding exclusion limits are more stringent. At the same time in dependence on θ_G the G' -boson with masses

$$m_{G'} > 2.55 \text{ (5.8) TeV} \quad (35)$$

is consistent with these data at $CL = 68\%$ and with masses

$$m_{G'} > 2.65 \text{ TeV} \quad (36)$$

at $CL = 90\%$ in the case of using the CT10 PDF set.

The CMS search [11] for dijet resonances was done at $\sqrt{s} = 8$ TeV with 19.7 fb^{-1} of the data and the dijet differential cross-section as function of the dijet mass was measured and is accessible at the HepData [12]. For comparison with CMS data we used in our numerical calculations the CMS dijet search criteria

$$\begin{aligned} |\eta_i| &< 2.5 \quad (i = 3, 4), \\ |\Delta\eta_{jj}| &< 1.3, \\ H_T &> 650 \text{ GeV}, \end{aligned}$$

where η_i is the pseudorapidity of each jet, $|\Delta\eta_{jj}| = 2|\eta_*|$ is the pseudorapidity separation of the two jets and H_T is the scalar sum of the jet p_T , and the values of the renormalization and factorization scales $\mu = \mu_R = \mu_F = p_T^{\max}$ and of the radius parameter $R = 1.1$.

By means of the programs MEKS and CalcHEP with using the CT10 and MSTW 2008 PDF sets we have calculated the dijet differential cross-sections (33) with account of the contributions of the SM NLO QCD and G' -boson in each dijet mass bin for the model parameters $m_{G'} > 1$ TeV and $10^\circ < \theta_G < 45^\circ$.

The comparison of the theoretical results with the CMS dijet data occurs to be slightly more complicated then that in the case of the ATLAS data.

In the upper left (right) section of the Fig. 3 we show the CMS data [11, 12] with their experimental errors by the solid lines and the dijet differential cross-section (33) calculated with accounting the SM NLO QCD contribution for the case of using the CT10 (MSTW2008) PDF sets by the dashed lines, for the jet radius parameter $R = 1.1$. In the corresponding lower sections of the Fig. 3 we show the relations $r_i = (\sigma_i^{\exp} - \sigma_i^{\text{th}})/\Delta\sigma_i^{\exp}$, where σ_i^{\exp} (σ_i^{th}) denote the experimental (theoretical) value of $\frac{d\sigma(pp \rightarrow \text{jet jet})}{dm_{jj}}$ in the i -th bin and $\Delta\sigma_i^{\exp}$ is the experimental error of this value, the dashed lines correspond also to the case of accounting only the SM NLO QCD contribution to σ_i^{th} .

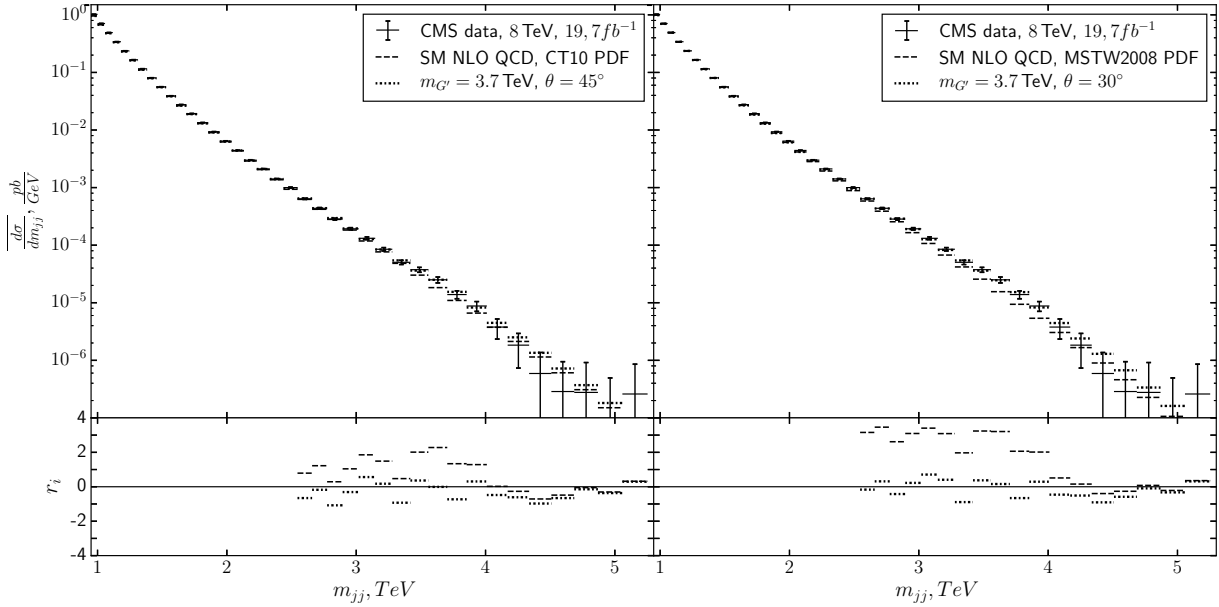


Figure 3: The dijet differential cross-section $\frac{d\sigma(pp \rightarrow \text{jet jet})}{dm_{jj}}$ calculated using the CT10 (MSTW2008) PDF set for the jet radius parameter $R = 1.1$ with account of the contributions of the SM NLO QCD and G' -boson with $m_{G'} = 3.7$ TeV, $\theta_G = 45^\circ$ ($m_{G'} = 3.7$ TeV, $\theta_G = 30^\circ$) in comparison with the CMS dijet data.

As seen from the Fig. 3 in the bins from the region $2.2 \text{ TeV} < m_{jj} < 4.0 \text{ TeV}$ the experimental values of the dijet differential cross-section exceed those calculated with accounting the SM NLO QCD contribution by more or about one experimental errors.

For the further analysis we use the last $N = 22$ bins of the Fig. 3 from the range $m_{jj} > 2.0 \text{ TeV}$. In this range the results of the SM NLO QCD calculations agree with the CMS dijet data with $\chi^2_{rSM} = 23.4/22 = 1.1$ ($\chi^2_{rSM} = 106.7/22 = 4.8$) in the case of using the CT10 (MSTW2008) PDF set. As seen, this agreement is not sufficiently good, especially in the case of using the MSTW2008 PDF set.

In the case of the simultaneous account of the contributions of the SM NLO QCD and G' -boson we vary two free parameters of the gauge chiral color symmetry model ($m_{G'}$ and θ_G) to minimize χ^2_r . It is found that in the case of using the CT10 (MSTW2008) PDF set the minimum of χ^2_r is at the values

$$m_{G'} = 3.7 \text{ (3.7)} \text{ TeV}, \quad \theta_G = 45^\circ \text{ (30°)}. \quad (37)$$

The dijet differential cross-section (33) calculated with simultaneous accounting the contributions of the SM NLO QCD and G' -boson with parameters (37) and the corresponding relations r_i are shown in the Fig. 3 by the dotted lines. This cross-section agrees with the corresponding CMS data (solid lines) with $\chi^2_{rmin} = 7.8/20 = 0.39$ ($7.2/20 = 0.36$) when using the CT10 (MSTW2008) PDF set, i.e. better in comparison with the quoted above $\chi^2_{rSM} = 1.1$ (4.8) in the case of accounting only the SM NLO QCD contribution (dashed lines).

We have found and analysed the exclusion and consistency $m_{G'} - \theta_G$ regions resulting from the CMS dijet data. In the lower sections of the Fig. 2 we show the excluded and allowed $m_{G'} - \theta_G$ regions resulting from the CMS data on the differential dijet cross sections

for $R = 1.1$ in the cases of using the CT10 (section c)) and MSTW 2008 (section d)) PDF sets. In these sections the crosses refer to the points (37) and the other notations are the same as those in the upper ones.

As seen from the Fig. 2 c), d) in the case of using the CT10 (MSTW 2008) PDF set the G' -boson for $\theta_G = 45^\circ$ (i.e. the axigluon) with the masses

$$m_{G'} < 3.35 \text{ (3.25) TeV} \quad (38)$$

is excluded at the probability level of 95% by the CMS dijet data and for the other values of θ_G the corresponding exclusion limits are more stringent. In the up-right part of the Fig. 2 d) there is an additional exclusion region but this region is caused mainly by the mentioned above not sufficiently good agreement between the CMS dijet data and the SM NLO QCD calculations with using the MSTW2008 PDF set. It is also seen that in the both cases c) and d) there are the $m_{G'} - \theta_G$ regions which are consistent with the CMS dijet data at $CL = 68\%$ and $CL = 90\%$.

It should be noted that our results are obtained with account only the G' -boson contribution to the dijet cross-sections and generally speaking the presence of the new particle (the exotic quarks an additional scalar particles) in the model could influence on these results.

Through their OCD interaction with gluons and interaction (13) with G' -boson the exotic quarks can contribute to the dijet cross-sections as well as give the analogous to (6), (7) additional contributions to the G' -boson hadronic width. We have calculated the contributions of the exotic quarks to the dijet cross-sections analogously to the case of the usual quarks and found that the CMS data [11, 12] are consistent within experimental errors with the existence of the exotic quarks with masses $m_{\tilde{q}'_{ia}} \gtrsim 900$ GeV. It is worthy to note that the current experimental low mass limits for additional heavy quarks are of about a few hundreds GeV. For example the ATLAS Collaboration excludes the t' quark with the mass $m_{t'} < 790$ GeV [18] and the CMS exclusion limit for $T_{5/3}$ is of $m_{T_{5/3}} < 800$ GeV [19].

Accounting in (6), (7) also the contributions of three generations of the exotic quarks with $m_{\tilde{q}'_{ia}} = 900$ GeV we obtain that the G' -boson peak becomes more wide and low, which slightly effects the results. For example instead of (38) we obtain in this case the mass limit $m_{G'} < 3.25$ (3.23) TeV, as seen the deviations are $\Delta m_{G'} = -100$ (-20) GeV. Because of (20), (18) the exotic quarks can be more heavy. For $m_{\tilde{q}'_{ia}} = 1.5$ TeV the deviations are small $\Delta m_{G'} \approx -(5 - 20)$ GeV and for $m_{\tilde{q}'_{ia}} > m_{G'}/2$ the effect of the exotic quarks on the the dijet cross-sections near the G' -boson peak becomes negligible.

As mentioned above the model under consideration reproduces in the scalar sector the SM Higgs doublet $\Phi_a^{(SM)}$ and predicts new colorless doublets Φ_a' and Φ_a'' and two doublets of color octets $\Phi_{ia}^{(1,2)}$. Although the SM Higgs doublet $\Phi_a^{(SM)}$ interacts with the SM fermions and W^\pm and Z bosons in the standard way the new doublets could contribute to the signal-strengths of the Higgs decays through the loop corrections. These loop contributions depend on the details of the interactions of the Higgs doublet with the new scalar doublets (coupling constants, mixings, masses). At the present time the signal-strengths of the partial Higgs decays are measured with accuracy of about 20 - 30 % [20]. For example the signal-strength is equal to $\mu_{H \rightarrow \gamma\gamma} = 1.17 \pm 0.27$ for the decay $H \rightarrow \gamma\gamma$ and has the global value $\mu = 1.18^{+0.15}_{-0.14}$. All the measured signal-strengths are compatible with the SM predictions. It seems that the uncertainty in the Higgs doublet interactions with the new scalar doublets allows at the present time to satisfy the current experimental values of the signal-strengths of the Higgs decays.

In conclusion, we summarize the results of this paper.

The possible contributions of G' -boson predicted by the chiral color symmetry of quarks to the differential dijet cross-sections in pp -collisions at the LHC are calculated and analysed in dependence on two free parameters of the model, the G' mass $m_{G'}$ and mixing angle θ_G .

Using the ATLAS [10] and CMS [11, 12] data on dijet cross-sections we find the G' -boson mass limits (in dependence on θ_G) imposed by these experimental data. In particular, it is found that in the case of using in theoretical calculations the CT10 (MSTW 2008) PDF set the G' -boson for $\theta_G = 45^\circ$ (i.e. the axigluon) with the masses

$$m_{G'} < 2.3 \text{ (2.6) TeV}$$

and

$$m_{G'} < 3.35 \text{ (3.25) TeV}$$

is excluded at the probability level of 95% by the ATLAS and CMS dijet data respectively. For the other values of θ_G the corresponding exclusion limits are more stringent. The $m_{G'} - \theta_G$ regions which are consistent with the ATLAS and CMS dijet data at $CL = 68\%$ and $CL = 90\%$ are also found. The possible effect of new fermion and scalar particles of the model on these mass limits is briefly discussed.

References

- [1] J. Pati, A. Salam, *Physics Letters B* **58**, 333337 (1975).
- [2] L. J. Hall, A. E. Nelson, *Phys. Lett.* **B153**, 430 (1985).
- [3] P. H. Frampton, S. L. Glashow, *Phys. Rev. Lett.* **58**, 2168 (1987).
- [4] P. H. Frampton, S. L. Glashow, *Phys. Lett.* **B190**, 157 (1987).
- [5] F. Cuypers, *Z. Phys.* **C48**, 639 (1990).
- [6] M. V. Martynov, A. D. Smirnov, *Mod. Phys. Lett.* **A24**, 1897 (2009).
- [7] M. V. Martynov, A. D. Smirnov, *Mod. Phys. Lett.* **A25**, 2637 (2010).
- [8] M. V. Martynov, A. D. Smirnov, *Phys. Atom. Nucl.* **75**, 321 (2012). [Yad. Fiz. 75, 349 (2012)].
- [9] I. V. Frolov, M. V. Martynov, A. D. Smirnov, *Mod. Phys. Lett.* **A28**, 1350035 (2013).
- [10] G. Aad, others [ATLAS Collaboration], *JHEP* **05**, 059 (2014).
- [11] V. Khachatryan, others [CMS Collaboration], *Phys. Rev.* **D91**, 052009 (2015).
- [12] *The Durham HepData Project*, <http://hepdata.cedar.ac.uk/view/ins1340084>.
- [13] C.G. Geng, *Phys. Rev.* **D39**, 2402 (1989).
- [14] A. Belyaev, N. D. Christensen, A. Pukhov, *Comput. Phys. Commun.* **184**, 1729 (2013).
- [15] J. Gao, *et al.*, *Comput. Phys. Commun.* **184**, 1626 (2013).

- [16] A. D. Martin, W. J. Stirling, R. S. Thorne, G. Watt, *European Physical Journal C* **63**, 189 (2009).
- [17] H.-L. Lai, *et al.*, *Phys. Rev.* **D82**, 074024 (2010).
- [18] The ATLAS Collaboration, ATLAS Note, ATLAS-CONF-2013-018.
- [19] S. Chatrchyan, *et al.*, *Phys. Rev. Lett.* **112**, 171801 (2014).
- [20] The ATLAS Collaboration, *European Physical Journal C* **76:6** (2016).